Characteristics and variability of the inner front of the southeastern Bering Sea

N.B. Kachel[a], G.L. Hunt Jr.[b], S.A. Salo[c], J.D. Schumacher[d],
P.J. Stabeno[c], T.E. Whitledge[e]

[a] *Joint Institute for Studies of Atmosphere and Oceans, University of Washington, Box 351640, Seattle, WA 98195, USA*
[b] *Department of Ecology and Evolutionary Biology, University of California at Irvine, Irvine, CA 92717, USA*
[c] *NOAA/PMEL, OERD2, Bldg. #3, 7600 Sand Point Way NE, Seattle, WA 98115-6349, USA*
[d] *Two Crow Environmental, Inc., P.O. Box 215, Silver City, NM 88062, USA*
[e] *School of Fisheries and Ocean Sciences, University of Alaska, P.O. Box 757220, Fairbanks, AK 99775-7220, USA*

Abstract

The inner front of the southeastern Bering Sea shows marked spatial variability in frontal characteristics created by regional differences in forcing mechanisms. Differences in forcing mechanisms (sea ice advance/retreat and storm strength and timing) and early spring water properties result in strong interannual variability in biological, chemical, and physical features near the front. We have developed a simple model based on surface heat flux and water-column mixing to explain the existence of cold belts (Cont. Shelf Res. 19(14) (1999) 1833) associated with such fronts. Hydrography, fluorescence and nutrient observations show that pumping of nutrients into the euphotic zone occurs, and this can prolong primary production at the inner front. The effectiveness of this process depends on two factors: the existence of a reservoir of nutrients in the lower layer on the middle shelf and the occurrence of sufficient wind and tidal energy to mix the water column.
© 2002 Elsevier Science Ltd. All rights reserved.

1. Introduction

Fronts that separate well mixed from stratified water columns are common features of shallow continental shelves. Because these fronts are a transition between different water column structures, they are often referred to as structural or structure fronts (e.g., Schumacher et al., 1979; Coachman, 1986). Alternatively, they are called tidal fronts since tidal mixing is the primary mechanism responsible for the vertical structure of the adjoining waters (e.g., Pingree and Griffiths, 1978; Franks and Chen, 1996). In a two-layered

stratified water column, tidal energy mixes the lower layer and wind-generated turbulence mixes the upper layer. Tidal fronts have been described in many locations: off the Amazon River (Geyer, 1995), on the Faroe shelf (Gaard et al., 1998), around the British Isles (Simpson and Hunter, 1974; Fearnhead, 1975; Pingree and Griffiths, 1978; Kasai et al., 1999), over Georges Banks (Franks and Chen, 1996; Chen and Beardsley, 1998), in the Yellow Sea (Lie, 1988), in the White Sea (Semenov and Luneva, 1999), and the Bohai Sea (Haung et al., 1999). Because of their impact on the distribution of temperature, salinity and baroclinic currents, tidal fronts influence the distribution of nutrients, phytoplankton, and

zooplankton (e.g., Franks and Chen, 1996; Gaard et al., 1998), and hence they influence the character of the ecosystem.

From late spring to fall, the inner front of the southeastern Bering Sea separates the well-mixed waters of the coastal regime from the two-layered system prevalent from over the middle shelf. The front is located in the vicinity of the 50-m isobath (Schumacher and Stabeno, 1998), but its position varies depending on wind and tidal strength (Overland et al., 1999). It extends for more than 1000 km starting near Unimak Pass, continuing around the perimeter of Bristol Bay, and then northwestwardly past Nunivak Island (Fig. 1).

Historical knowledge of the inner front is based on limited sets of observations. The first description of the hydrographic structure of the front was based on a single transect in the vicinity of Nunivak Island (Muench, 1976). Observations collected between 1976 and 1978 as part of the Outer Continental Shelf Environmental Assessment Program (OCSEAP/NOAA) provided the first general characterization of the inner front (Schumacher et al., 1979; Kinder and Schumacher, 1981). These studies suggested that the inner front was 5–12 km wide and that its position was a function of the slope of the sea floor. More data were collected between 1978 and 1982, as part of
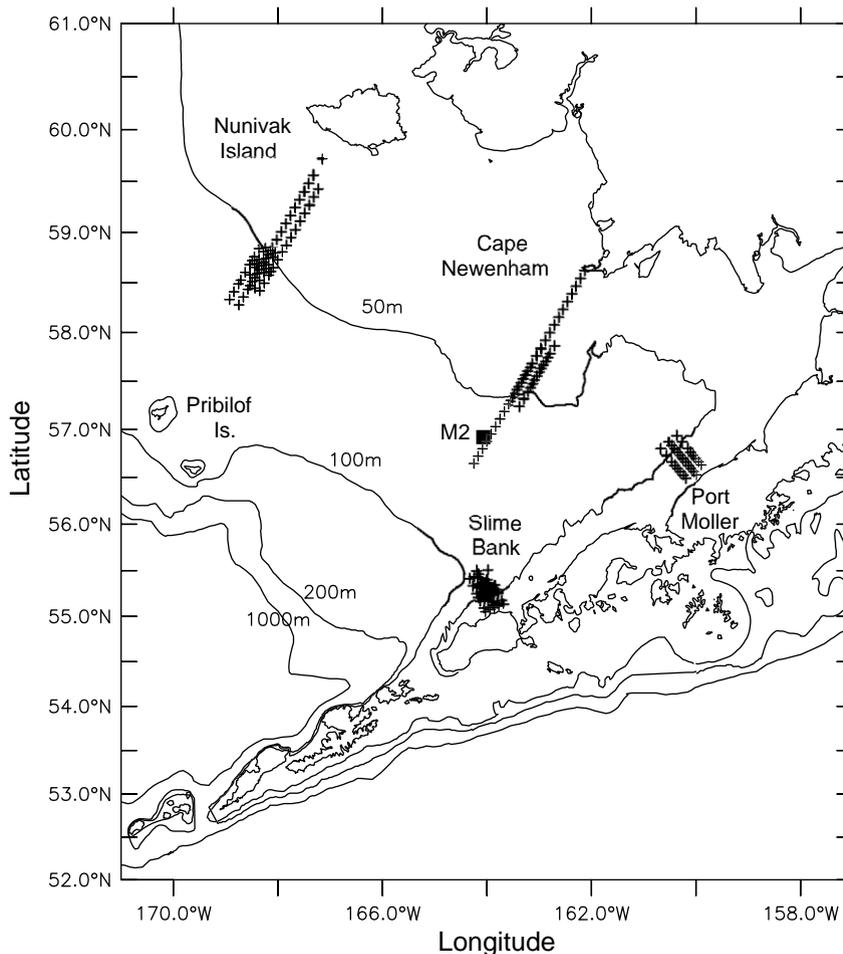
Fig. 1. The southeastern shelf of the Bering Sea showing names and locations of CTD stations; M2 is the site where continuous biophysical observations are collected (Stabeno et al., 2003). Depth contours are in meters.

the Processes and Resources of the Bering Sea Shelf (PROBES, National Science Foundation (NSF)) study, added details about frontal locations, seasonal and interannual variability, and the gradients of temperature and salinity, as well as nutrient and chlorophyll distributions across the inner front (Whitledge and Walsh, 1986). Kinder et al. (1983) demonstrated the existence of a
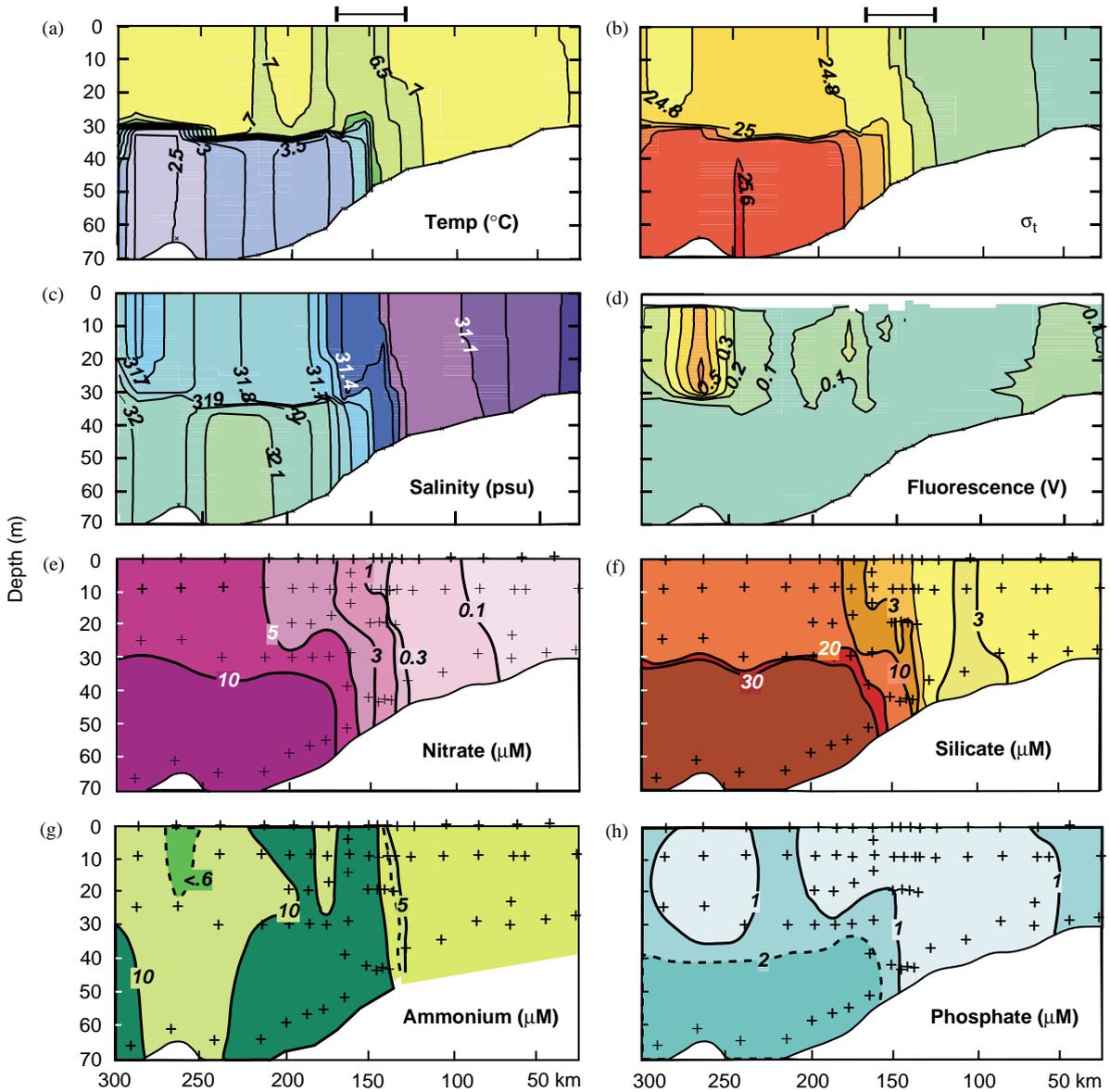
Fig. 2. Features of the coastal and middle-shelf domains, as well as inner front along a transect from Nunivak Island towards the Pribilof Islands (29–30 August 1998). (a) Isotherms (note the bottom water region with $T < 2.5°C$ over the middle shelf, which is known as the cool (cold) pool, and the well-mixed waters of the coastal domain), (b) isopycnals in units of $10^3 \, kg \, m^{-3}$, (c) isohalines (psu), (d) relative fluorescence (V), as well as (e) isopleths of nitrate (μM), (f) silicate, (g) phosphate, and (h) ammonium, all in units of μM. Distances are measured from the coast. Bars at the top of the page mark the position of the inner front. Positions of nutrient samples are shown by plus signs.

structural front around the Pribilof Islands, and found higher densities of feeding seabirds there as did Decker and Hunt (1996). This led to the hypothesis that the inner front of the Bering Sea is a zone of enhanced vertical flux of nutrients and prolonged production (Hunt et al., 1996).

A particularly long (~ 300 km) transect of water properties (Fig. 2) illustrates salient features of the middle shelf domain, the inner front, and the coastal domain. Stratification over the middle shelf is primarily a result of summer heating, although in years with late melting of sea ice, salinity can contribute to vertical structure. When the bottom layer over the middle shelf has temperatures $< 2.0°C$, it is known as the cold pool (Takemouti and Ohtani, 1974). Variations in timing and distribution of ice over the shelf in winter and spring cause the extent and minimum temperature of the cold pool to vary greatly from year to year (Schumacher and Stabeno, 1998). In years with an early ice retreat, such as 1998, the summer temperature of the coldest bottom waters is between 2°C and 5°C and is referred to as "cool pool." Nutrient concentrations in summer are greatest within or near the cold (cool) pool (Hattori and Goering, 1981; Whitledge and Luchin, 1999). During the summer, the coldest surface waters are consistently found near the shoreward edge of the inner front. In Fig. 2, this appears as the ~ 40 km wide band of water with temperatures $< 6.5°C$. The term "cold belt" has been applied to similar features described by Haung et al. (1999) for the Bohai Sea, and we use that term herein.

The dynamics associated with the inner front and in particular with the cold belts have an important impact on nutrient distributions and hence on phytoplankton productivity. Enhanced production at the front would be expected to attract large numbers of upper trophic level animals. The hypothesis that prolonged primary and secondary production occur at the inner front of the eastern Bering evolved from observed distributions of feeding short-tailed shearwaters (Hunt et al., 1996), and was the basis for the NSF supported Inner Front research project. In this manuscript, we present conductivity/temperature/ depth (CTD), fluorescence and nutrient data from

Table 1
Number of CTD stations occupied on the inner front grids during each cruise

Cruise ID	Date	No. of CTD casts
HX196	29 May–28 June 1997	230
HX200	27 Aug–12 Sept 1997	126
HX209	23 May–24 June 1998	253
HX213	15 Aug–6 Sept 1998	135
HX220	17 May–18 June 1999	247
HX222	18 July–22 Aug 1999	214
Total	1997–1999	1205

1997, 1998, and 1999 that were collected during the Inner Front Project (IFP) cruises (Table 1). Our goal is to refine our knowledge of the temporal and spatial variability of water property characteristics associated with the inner front.

2. Methods

During the IFP cruises, we occupied four grids of transects at Nunivak Island, Cape Newenham, Port Moller, and Slime Bank (Fig. 1). Each grid contained a core of 2–5 transects of CTD stations spaced 5 km apart. Extending beyond the central core of 10–12 stations on each line, additional stations were spaced 10–20 km apart. In the central core of stations, the time between successive stations was ~ 25 min. Data were obtained using a SeaBird 911-Plus CTD with dual temperature and conductivity sensors and fluorescence was measured using a Wetlabs fluorometer. Data were recorded on downcasts, at a descent rate of 15–30 m min^{-1}. To provide salinity calibrations, near-bottom water samples were taken at approximately every second cast. These calibrations suggest instrument accuracy better than 0.01 practical salinity units (psu). The use of dual sensors reduced the number of data gaps, particularly in the Slime Bank region, where jellyfish posed significant problems for conductivity measurement. The problem of biological fouling of the CTD typically occurred as the instrument was lowered through the pycnocline. In such instances salinity data were lost from the bottom half of

casts. In the late spring to early fall, when an inner front may exist on the eastern Bering Sea shelf, temperature differences have a greater effect on density than do salinity differences. For example, in June and August 1997, temperature differences at sites with stratification typically accounted for about 75% of the density difference between the surface and the bottom waters. Where salinity had

a greater effect, the halocline and thermocline were at the same depth. Therefore, temperature data provided the most complete and accurate description of the physical structures.

Water samples were collected at almost every station on the central transects for analysis of nutrient content. Nutrient samples were collected using polyethylene vials, pre-washed with dilute
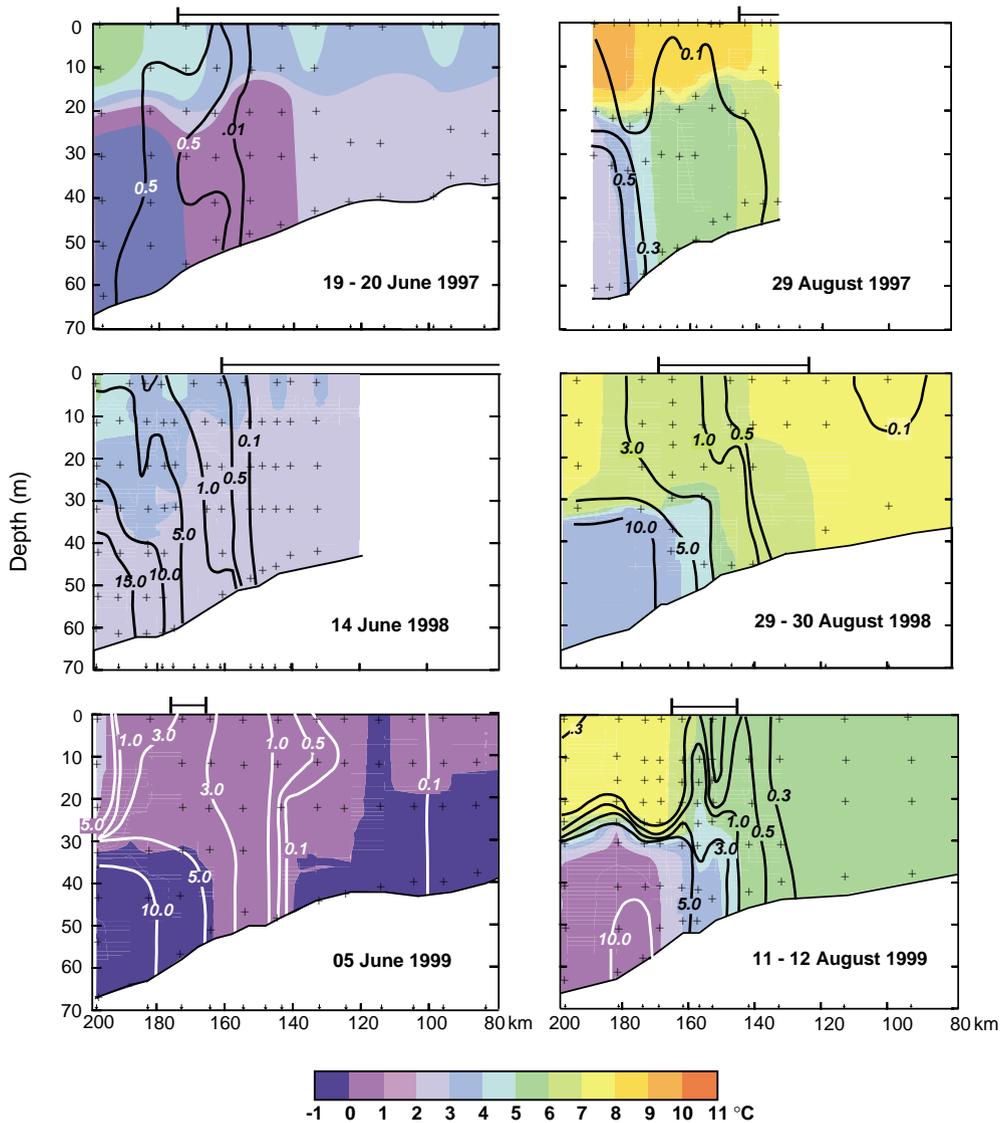
Fig. 3. Transects of temperature (colors) and nitrate (contours) off Nunivak Island. CTD stations are marked along the bottom axis. Positions of nutrient samples are shown by plus signs. Distances are measured from the coast. Bars at the top of each frame mark the calculated positions of the inner front.
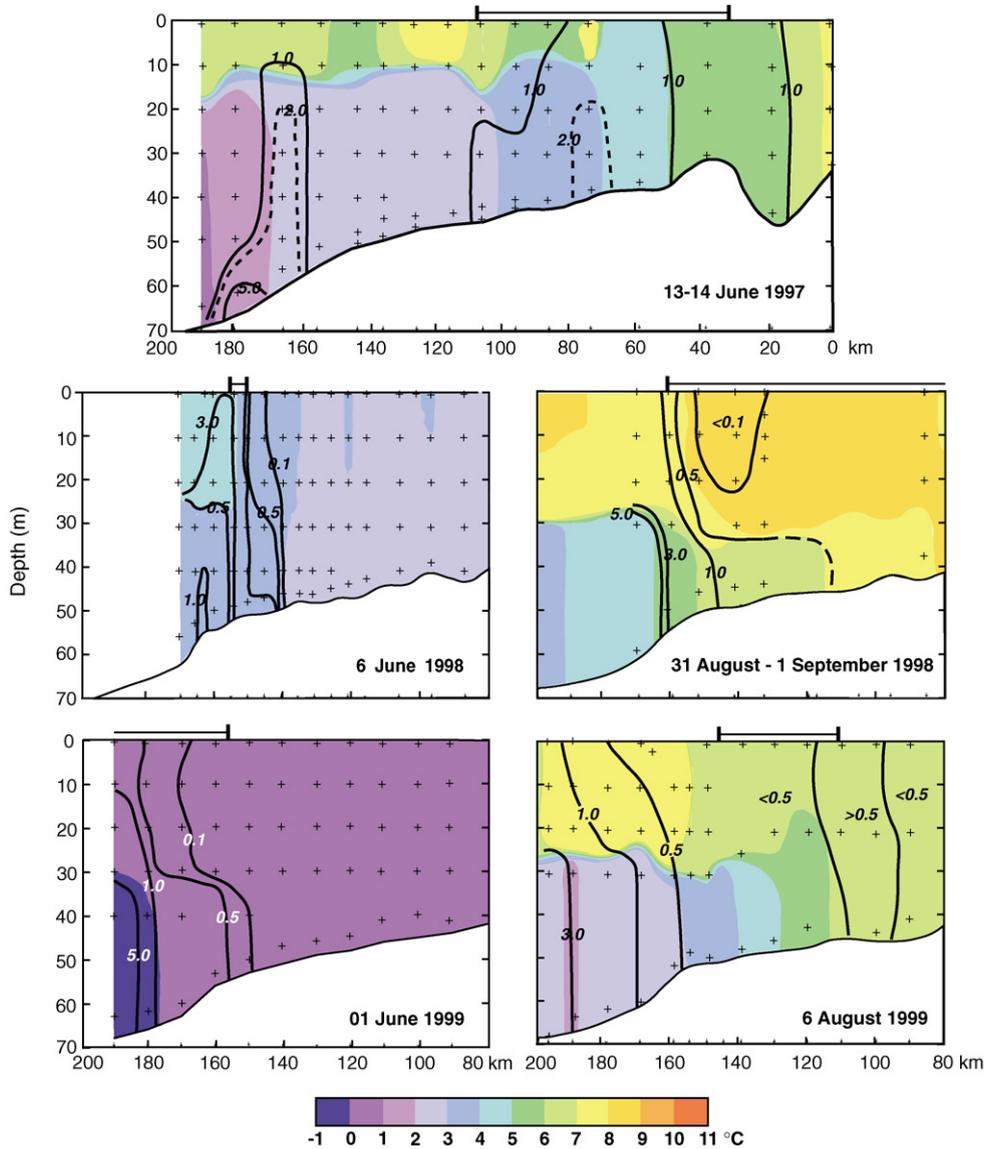
Fig. 4. Transects of temperature (colors) and nitrate (contours) off Cape Newenham. CTD stations are marked along the bottom axis. Positions of nutrient samples are shown by plus signs. All sections have the same horizontal scale. Distances are measured from the coast. A bar at the top of each frame marks the calculated position of the inner front.

HCl, and triple rinsed with sample water. Samples were stored upright in a refrigerator until they were processed using an onboard Alpkem Model 300 automated nutrient analyzer (Whitledge et al., 1981). The distribution of nutrient samples is indicated by plus signs in the temperature/nutrient sections (Figs. 2–6).

3. Description of the inner front

3.1. Relationship among water properties

The long transect between Nunivak Island and the Pribilof Islands provides an example of the structure of the inner front (Fig. 2). It was
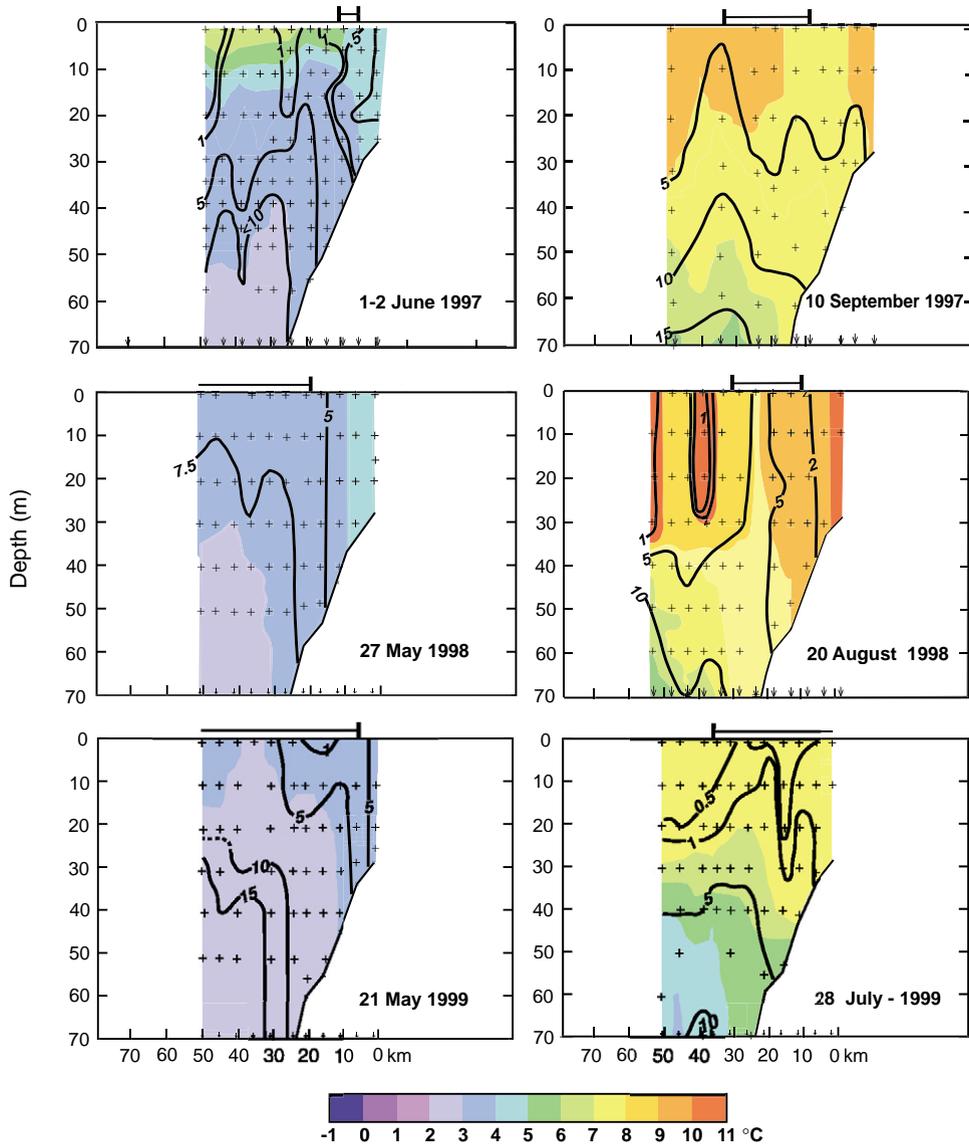
Fig. 5. Transects of temperature (colors) and nitrate (contours) off Slime Bank. CTD stations are marked along the bottom axis. Positions of nutrient samples are shown by plus signs. Distances are measured from the coast. Bars at the top of each frame mark the calculated positions of the inner front.

occupied in August 1998 after mixing by a storm replenished nutrients in the upper layer of the water column. A region of elevated fluorescence was present over the cool pool. Several transects on this study indicated a second, less pronounced area of elevated values, over the shoreward portion of the inner front. Concentrations of nitrate, silicate, and phosphate were high in the stratified area, in contrast to the depleted levels in the coastal domain. Patterns of distribution for silicate and phosphate were similar, though not identical in details, to those of nitrate. In general, there were higher nutrients in the lower layer of the middle shelf (cool pool) and reduced nutrients in
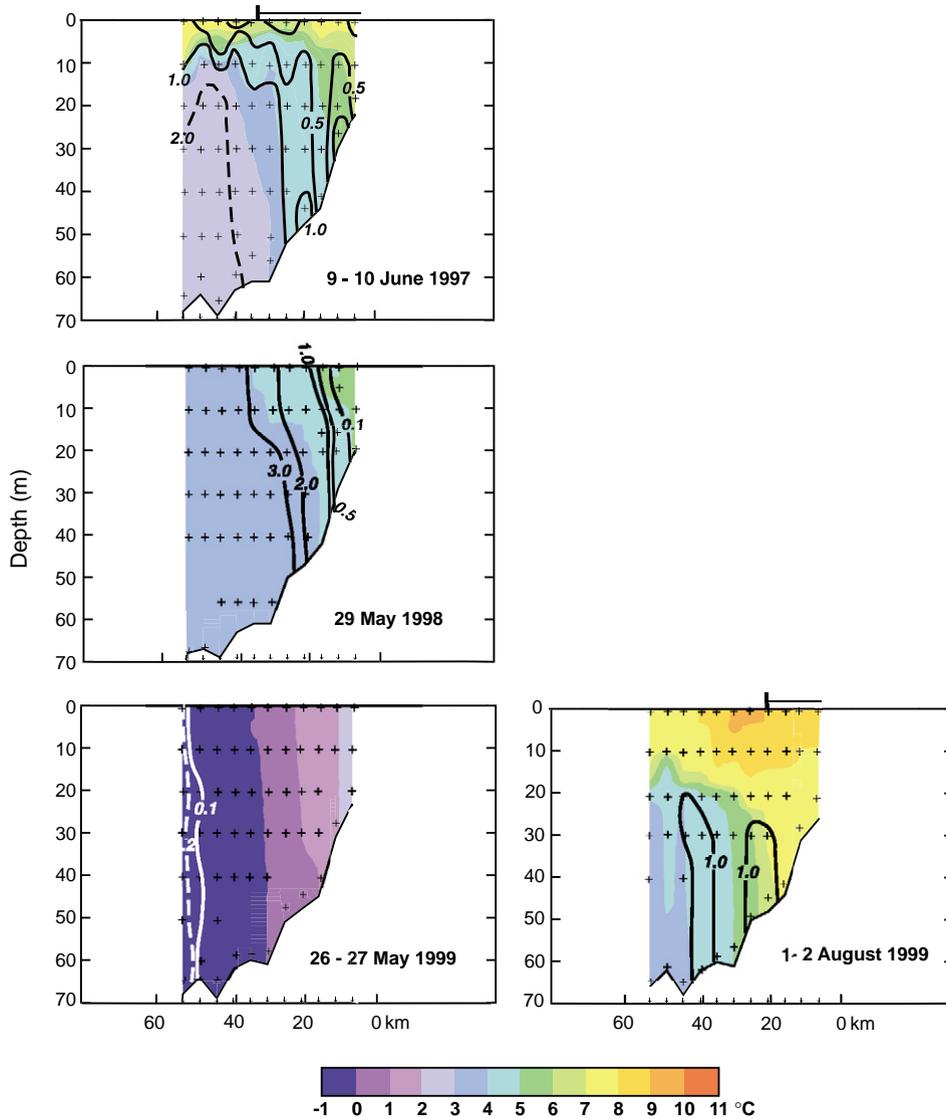
Fig. 6. Transects of temperature (colors) and nitrate (contours) off Port Moller. CTD stations are marked along the bottom axis. Positions of nutrient samples are shown by plus signs. Distances are measured from the coast. Bars at the top of each frame mark the calculated positions of the inner front.

the upper layer. The difference is likely a result of biological uptake and remineralization of the elements. It should be noted that the nutrient concentrations on this transect were among the highest we measured. The distributions of nitrate, silicate, and phosphate had vertical filaments or regions of higher concentration at shallower

depths at the front that indicate movement from the lower layer into the upper at a location coincident with the coldest sea-surface temperatures (SST). We infer that phytoplankton biomass (indexed by the high fluorescence) may have decreased phosphate concentrations over the cool pool. The ammonium distribution also suggests

biological draw-down of nutrient concentrations in the middle shelf regime, especially in the upper layer.

For the purpose of elucidating the physical/chemical processes at the inner front, the distribution of nitrate appears to be the best chemical marker to identify mixing and replenishment processes critical to sustained summer production. Therefore, we present temperature transects from each grid area in color together with contours of nitrate concentration to illustrate the relationship between nutrients and the temperature (density) structure of the water column.

3.2. Seasonal and interannual variability—Nunivak Island and Cape Newenham Lines

The most complete description of both seasonal (early to mid June versus mid to late August) and interannual (1997–1999) changes associated with the inner front was provided by observations off Nunivak Island (Fig. 3) and Cape Newenham, which approximates the main PROBES line (Fig. 4). The depth and intensity of the thermocline over the middle shelf, the temperature profiles, the width of the inner front, and its distance from the coast were all markedly variable. During June 1998 and 1999, the distribution of isotherms indicated that warming over the cold/cool pool had just begun. Vertical and horizontal gradients of temperature were weak and the front was broader than typical. In 1997, the warmer surface layer ($T > 4.5°C$) off Nunivak Island (Fig. 3) was more extensive and shallower than in other years and the inner front had already been established by mid-June. Stabeno et al. (2001) observed that the well-mixed coastal domain was less extensive than that observed in any other year. By August 1997, the warmest surface temperatures were 2–3°C greater than during 1998 or 1999, and the depth of the thermocline was 10–13 m shallower than in subsequent years. This interannual pattern was also evident off Cape Newenham (Fig. 4) and was consistent with previous results (Stabeno et al., 2001; Schumacher et al., 2002). A combination of moderate winds and reduced cloud cover led to extremely warm SSTs in 1997. During 1998, both June and August transects off Cape Newenham showed increased bottom temperatures and cooler SSTs than in 1997. The failure of sea ice to cool the water column to near freezing during early spring resulted in a water column with greater heat content (2°C higher average temperature) in 1998 than in 1997 (Stabeno et al., 2001). In 1999, the late retreat of sea ice resulted in the coldest bottom temperatures of the three years (Figs. 3 and 4).

In June 1997 at the shoreward edge of the inner front near Cape Newenham, an ~10 km wide band of colder water (cold belt, 4–5°C) extended from the bottom to the surface, separating the warmer water extant over the middle shelf and the coastal domain (6–8°C) (Fig. 4). Cold belts were also observed at Nunivak Island and Slime Bank (Figs. 3 and 5; and the Appendix A).

A time series of fluorescence recorded at site M2 (Fig. 1) in 1997 indicated an early phytoplankton bloom associated with the ice edge (Stabeno et al., 2001), which would have drawn down nutrient concentrations in the surface layer. Nutrients were subsequently resupplied from the bottom layer by a May storm that mixed nutrients from the cold pool into the upper water column, after which a second phytoplankton bloom was observed (Stabeno et al., 2001). By June, nutrients were depleted on both the Nunivak and Newenham grids ($NO_3 < 1.0 \,\mu M$). By early August, the surface layer was the warmest ever recorded (Stabeno et al., 2001). Our transects showed that this sequence of events occurred over a large portion of the southeastern Bering shelf. The early water column stability, shallow thermocline, and nutrient depletion in 1997 stands in marked contrast to the water column characteristics during the stormier conditions in 1998 (Stabeno et al., 2001). In 1998, storms created a deeper mixed layer and isolated a reservoir of nutrients in the bottom layer over the middle shelf. In 1999, late ice melt followed by surface heating again isolated nutrients below the thermocline, establishing a nutrient reservoir for the replenishment processes at the inner front. The clearest example of this process of introducing nutrients at the inner front occurred on the Nunivak Island grid during August 1999, and was also evident, albeit less dramatically, in August 1998 (Fig. 3).

3.3. Spatial variability—comparison with Slime Bank and Port Moller

Along the Alaskan Peninsula, the relatively straight coastline and narrow coastal domain permits wind-driven divergence and fresh-water discharge to be important to regional dynamics (Coachman, 1986; Schumacher and Stabeno, 1998). An example of the impact of wind-driven coastal divergence is inferred from temperature distributions off Port Moller (June 1997, Fig. 6). For a 48-h period prior to the occupation of this transect, the wind had a mean alongshore component of $\sim 4.0\,\mathrm{m\,s^{-1}}$ towards 225°T. In response, a warm shallow tongue of fresher coastal water ($T > 7.0$°C) was transported offshore ~ 10 km, overrode the inner front, and thus hindered the upward mixing of waters there. Similar wind events are common along the peninsula, which suggests this feature may be common in summer along the peninsula. Another feature of this region is the presence of a northeastwardly flowing current, whose source is Unimak Pass and Bering Canyon (Schumacher et al., 1982; Stabeno et al., 2002). This current can transport water along this portion of the inner front and has an important impact on the distribution of water properties there.

The feature that primarily distinguished transects at Slime Bank (Fig. 5) and Port Moller (Fig. 6) from those at Nunivak Island (Fig. 3) and Cape Newenham (Fig. 4) was the absence of the sharp thermocline. With some exceptions (June 1998 and May 1999 at Port Moller, and June 1998 at Slime Bank), cold belts were evident in transects off the Alaskan Peninsula. Increased nitrate concentrations coincided with these features. Transects at Slime Bank, closest to the head of Bering Canyon—a potential source of slope water with high levels of nutrients (Stabeno et al., 2002)—had the highest levels of nutrients. The temperature structure in July 1999 had a pattern typical of upwelling conditions. By contrast, at Port Moller surface-layer nutrients were close to depletion all four times we sampled there, while the bottom and offshore waters also had lower concentrations of nutrients than observed at Slime Bank. Twice, plumes of warm water from near the coast overlaid the area, inhibiting vertical mixing. Overall, the transects near the Alaskan Peninsula showed stronger horizontal gradients and reflected their proximity to both slope water and to warmer, less saline water from land.

3.4. Definition of the position of the inner front

To characterize the inner front, an objective definition of its location was needed. Prior researchers proposed that structure fronts are located where the ratio of water-column depth to tidal current speed attains a given value. For example, for the Clyde Sea front Kasai et al. (1999) found its position where $\log_{10}[H/U_2^3] = 2.7-3.7$, where H is the bottom depth and U_2 is the amplitude of the M2 tidal current. Over the Bering shelf, the uncertainty in this formulation yields results too widely spread to be useful. Schumacher et al. (1979) used a first difference scheme that consisted of the horizontal gradient of the temperature difference between upper and lower layers based on XBT observations collected at an approximately 1 km separation. The practical difficulty of this definition is the need for densely distributed data—a particular problem on such a wide shelf, where the position of the front was seen to vary dramatically both seasonally and interannually. It is clear that a new definition is needed.

The present study included 83 occupations of 15 transects in four geographically different areas. From visual inspection it is evident that the position of the inner front changed on seasonal, interannual, and tidal timescales. The grid spacing of the stations plus the variety of conditions sampled made it possible to find an improved definition of the frontal end points based on hydrography alone. We use the fact that, during summer, the water column over the middle shelf consists of two distinct layers separated by a sharp thermocline (e.g., Coachman, 1986). The transition from the two-layered system to the inner front begins where the temperature gradient at the thermocline begins to weaken. So, the offshore endpoint of the inner front is defined here as the location where the maximum value of $|\mathrm{d}T/\mathrm{d}z|$ becomes less than one-half the greatest value

observed on that grid of stations. An additional constraint imposed is that $|\mathrm{d}T/\mathrm{d}z| < 1^{\circ}\mathrm{C}\,\mathrm{m}^{-1}$, which eliminated spurious positions associated with certain wave-like structures along the thermocline over the cold (cool) pool. At the nearshore end of the front the waters of coastal domain water are nearly unstratified. Therefore, the inshore position is defined as the seaward-most location with the maximum $|\mathrm{d}T/\mathrm{d}z| < 0.05^{\circ}\mathrm{C}\,\mathrm{m}^{-1}$.

Using this method, 34 CTD transects were identified that contained both ends of the front (see Table 2). On the Cape Newenham and Nunivak Island transects, the average width of the front was 40 km, with a range of 5–127 km. On the Slime Bank and Port Moller transects, the average frontal width was 19 km, with a range from 2 to 34 km. The average distance from the coast to the inner edge of the front off Nunivak Island and Cape Newenham was 126 km, with a range of 29–169 km. By comparison the average distance off the Alaskan Peninsula was 14 km, with a range of 5–39 km. In addition to the locations of the inner front on each transect, Appendix A lists the temperature and salinity of the surface and bottom waters over the middle shelf regime, the depth of the thermocline over the cold pool, as defined by the maximum value of $\mathrm{d}T/\mathrm{d}z$, and the minimum SST along the transect (cold belt temperature) are also presented. All positions are measured as distances from the coast.

The width of the inner front at Nunivak Island and Cape Newenham can be so broad that the name "front" is no longer meaningful. It seems more appropriate to call this feature a transition zone. From examination of all the IFP transects, a width exceeding $\sim 45\,\mathrm{km}$ defines a transition zone. The three transects in Fig. 9 represent times when an active inner front is present, while the transects shown at Nunivak Island in 1997 and in June 1998 would be described as having transition zones. Occasions when transition zones were observed coincided with times of both low wind speeds and low tidal amplitudes, in comparison to times when narrower fronts were found.

Schumacher et al. (1979) suggested that an inverse relationship existed between the slope of the sea floor and width of the front (the greater the slope the narrower the front). Sea-floor slopes along the Alaska Peninsula are an order of magnitude steeper than slopes on the Nunivak Island and Cape Newenham grids, yet frontal widths along the Alaskan Peninsula were within the range of values observed on the broader shelf to the north (Appendix A). Overall, our data showed poor statistical correlation between bottom slope and frontal width. The calculated widths of the inner front on the Slime Bank and Port Moller grids tended to decrease with increasing bottom slope, but those on the Nunivak Island and Cape Newenham grids bore no relationship to the bottom slope.

Highly variable conditions among the years of the IFP limited the number of times that both sides of the front were observed during the IFP cruises. This was especially true during 1997, when a warm surface layer extended far inshore of the expected $\sim 50\,\mathrm{m}$ isobath position indicated by previous studies. Stormy conditions in the late spring of 1998 and the late retreat of the sea ice in 1999 meant that the inner front was just beginning to be set up during the spring cruises of those years (Table 1). The grid areas along the Alaskan Peninsula are influenced by both nearshore freshwater plumes, and by advection of more oceanic water eastward from Unimak Pass. These factors inhibit the development of a well-mixed coastal zone and a two-layered middle-shelf regime, respectively. Therefore, a fully developed inner front is less likely to occur there. In conclusion, this study revealed that frontal position was highly variable and sensitive to forcing mechanisms.

4. Features associated with the inner front

4.1. Cold belts

Although cold belts (Haung et al., 1999) were not discussed in the earlier literature on the eastern shelf of the Bering Sea, they were evident in the earlier data sets. For example, a band of cooler water ($< 7.0^{\circ}\mathrm{C}$) just shoreward of the inner front was shown in a transect occupied in 1974 (Muench, 1976). Such bands are also apparent in nutrient distributions collected between 1978 and 1980 (Whitledge and Walsh, 1986).

The origin of the cold belts can be explained by examining the depth to which mixing distributes the net surface heat flux through the water column. In the typically unstratified coastal domain, net surface heating is distributed throughout the entire water column by mixing. As depth increases away from the coast, the same quantity of surface heat is mixed down into increasingly greater depths, resulting in cooler temperatures. Over the two-layer middle shelf regime, that same heat warms only the upper mixed layer. This results in warmer temperatures above the thermocline than in the coastal regime adjacent to the inner front.

During the early summer, when advection is weak (Schumacher and Kinder, 1983; Stabeno et al., 2001), water temperatures on the shelf depend mainly upon their initial temperature in the spring and the net surface heat exchange, Q_t. This quantity is the difference between solar radiation input and loss due to net long-wave radiation, latent heat losses due to evaporation, and sensible heat loss (Reed and Stabeno, 2003). Typically, in the southeastern Bering Sea, the initial temperature, T_0, at the beginning of the season is constrained by the freezing temperature of seawater (approximately $-1.7°C$). Using data for May–July on the Bering Sea shelf, Reed and Stabeno found good correspondence between the estimates of net heat exchange across the surface and the heat content of the water column, H (in $W\,m^{-2}$), as calculated by

$$H = \rho c_p \int T \, dz \qquad (1)$$

in which ρ is seawater density, c_p is the specific heat of seawater at constant pressure ($\sim 4\,J\,g^{-1}\,°C^{-1}$), T is water temperature ($°C$), and z (m) is the vertical axis. In this analysis, H is referenced to T_0, the water temperature on April 15 or after the sea ice retreats, whichever comes last. Therefore, H is a relative heat content in the water column. Where the water column is well mixed, SST can be used for T, and Eq. (1) can be rewritten as

$$T - T_0 = f(Q_t/h) = Q_t/\rho c_p h \qquad (2)$$

in which Q_t ($W\,m^{-2}$) is the net heating that has occurred to date from the beginning of the spring

season, h is the water depth, and T_0 is the initial temperature in early spring.

As an example, this formulation was applied to the data at the inshore end of Nunivak Island grid in June 1997 and in August 1999 in the region inshore of the two-layered system (found at a depth less than 57 m in August 1999). A second-order Taylor series expansion centered at 36 m depth was constructed for the function, and resulting coefficients were compared to those calculated by a second-order polynomial fit of SST to bottom depth (Fig. 7). Minimizing the differences between sets of corresponding coefficients, suggested that over the period from 15 April to 20 June 1997, $Q_t = 148\,W\,m^{-2}$ and $T_0 = -0.5°C$ on 15 April. The results for a similar
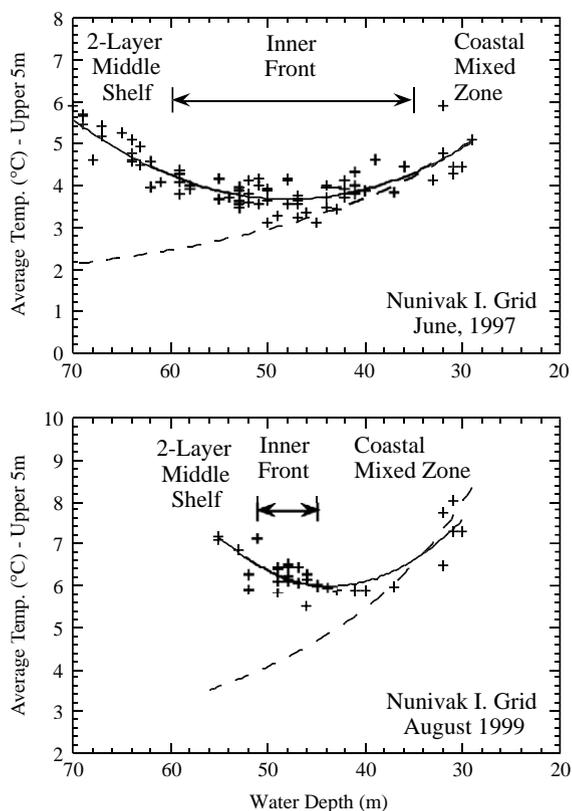
Fig. 7. Regression of SST vs. bottom depth for all stations taken on the Nunivak Island grid during June 1997, $R = 0.67$ (top), and August 1999, $R = 0.82$ (bottom). The dashed lines are the temperatures predicted by the expression $T = T_0 - Q/h$ in the absence of the formation of a two-layer regime.

calculation for the period from 1 May to 12 August 1999 were that $Q_t = 286 \, \mathrm{W \, m^{-2}}$ and $T_0 = -1.65°\mathrm{C}$ at the time the last ice retreated. For comparison, Reed and Stabeno (2003) estimated the average monthly net surface heat flux at Site M2 (Fig. 1) from May to July 1996 as $142 \, \mathrm{W \, m^{-2}}$. The results from the simple estimate made here were somewhat lower than their estimate would predict (if extrapolated over the longer time period of our calculations). This likely indicates that advection had occurred.

A fit of $T = (T_0 - Q_t/h)$ plotted on the same graphs (Fig. 7) show the temperatures that would result if there were no stratification over the two-layer regime. When wind and tide conditions move the inner front seaward, mixing of cold water from below the thermocline with warmer upper-layer waters would cause the temperatures of the water column across the deepening shelf to approach those predicted by Eq. (1).

4.2. Variability due to storms

Storms have a pronounced influence on characteristics of the inner front. We were able to observe the following case near Nunivak Island. Transects were occupied before and after the passage of a storm (31 August–1 September 1997) (Fig. 8). We used NCAR/NCEP Reanalysis winds to calculate (wind stress)$^{3/2}$, an index of mixing. This parameter increased 30%, from ~ 0.1 to $0.13 \, \mathrm{N \, m^{-2}}$ for a period of 2.5 days before returning to pre-storm levels (inset, Fig. 8). Before the storm, the two-layered regime extended across the entire transect, the upper mixed layer was $\sim 15 \, \mathrm{m}$ deep and SSTs exceeded $10°\mathrm{C}$ (Fig. 8, top). Although the transect shown here did not pass through the shoreward end of the front, the position of the front on the nearby transect (NIE, 15 km to the northwest) was found between 105 and 153 km from the coast (see Appendix A). After the storm, the mixed layer had deepened to greater than 20 m, SSTs over the cold pool had decreased by $\sim 2.0°\mathrm{C}$, and the outer edge of the front had moved offshore ($\sim 20 \, \mathrm{km}$) (Fig. 8, bottom). As the inner front moved offshore, the well-mixed region of the coastal zone widened and a cold belt (7.0–7.5°C) formed. The temperature in that area was 0.5–1.0°C less than the pre-storm temperatures on the line to the northwest.

4.3. Comparison of three successive transects of Nunivak Island in August 1999

In August 1999 we occupied one transect on the Nunivak Island grid three times within 5 days (Fig. 9). These transects began one week after a storm with an index of wind mixing more than 3 times greater than we saw while we were there. The first transect was occupied just after the maximum in tidal mixing associated with a spring tide. The coastal domain waters were uniformly between 5.5°C and 6°C, while upper-layer waters over the middle shelf were generally between 7°C and 7.5°C. Within 5 days both of these regions had warmed by $\sim 0.5°\mathrm{C}$. The top panel represents the same transect presented in Fig. 3, in which elevated concentrations of nitrate coincided with the humps in the 5.5°C contour. The second panel shows a transect through the area 2 days later with half the distance between stations (2.5 km). A wave-like feature, marked by the 6.0°C isotherm, was observed with a height of $\sim 10 \, \mathrm{m}$. On the third transect a series of humps or wave-like features represent a vertical movement of 10–20 m of colder, more nutrient-rich water from below. Moored instruments nearby recorded similar vertical excursions of the thermocline.

While the mechanism that causes these wave-like features is unknown, similar features were observed on Georges Bank (Loder et al., 1992). There, they were the result of internal tides. These features could play an important role in supplying nutrients for primary production by bringing nutrient-rich water nearer the surface where storms could then easily mix those nutrients into the euphotic zone.

4.4. Nutrient enrichment at the inner front

The hypothesis of the IFP was that the inner front is a site of prolonged primary production during summer in the Bering Sea (Sambroto et al., 1986; Hunt et al., 1996). If true, the front could provide a persistent source of food to higher trophic levels that would extend throughout the
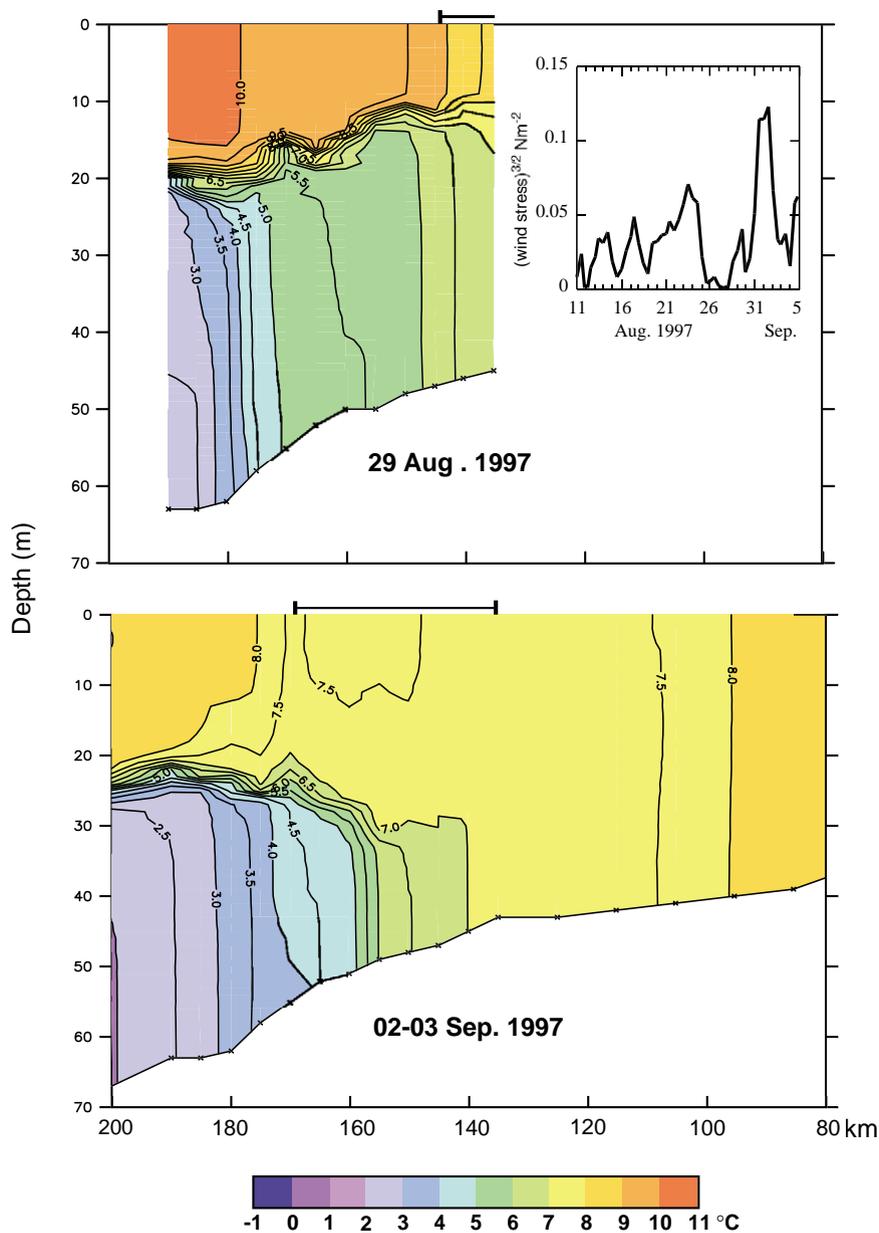
Fig. 8. Transect of temperature off Nunivak Island before (top) and after (bottom) a storm. Contour interval is 0.5°C. The insert shows a time series of (wind stress)$^{3/2}$, a measure of mixing energy, computed from NCAR/NCEP Reanalysis synthetic wind speed. Bars at the top of each frame mark the calculated positions of the inner front.

summer. For this to occur, nutrients must be introduced. By early summer nutrients in the coastal zone and the waters of the euphotic zone over the shelf usually are exhausted, but a large reservoir usually exists below the euphotic zone.

The most likely mechanism for the introduction of nutrients into the euphotic zone is wind mixing (Sambroto et al., 1986; Whitledge et al., 1986; Hunt et al., 1996). A striking example of this process was observed after a storm in August 1999
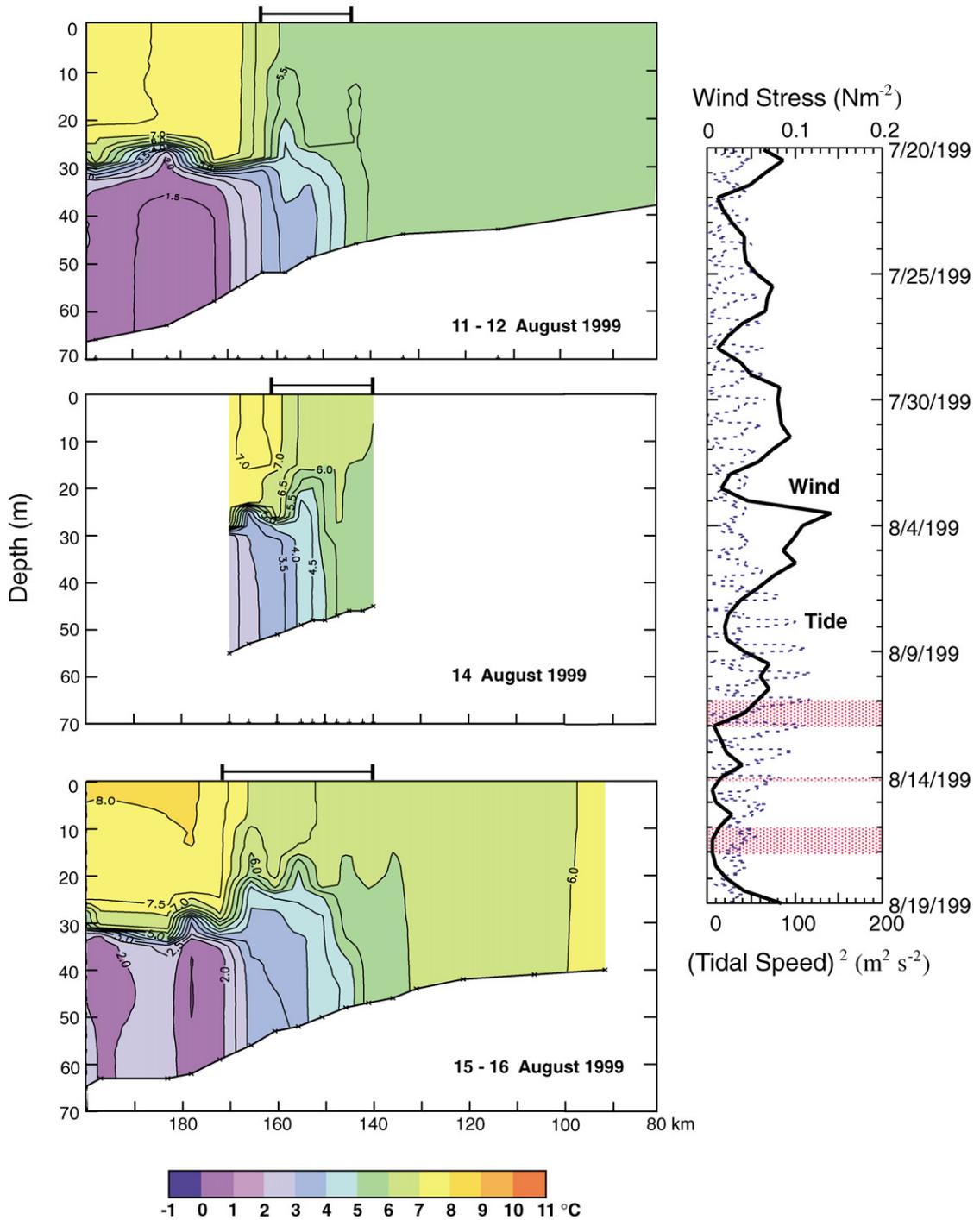
Fig. 9. Three transects of temperature across the inner front at the Nunivak Island showing wave-like features of colder bottom water from the middle shelf extending into the inner front zone. The panel to the right shows (wind stress)$^{3/2}$ and (tidal speed)^3, measures of mixing energy, before and during the transects. On August 3, 1999 storm winds exceeded $14\,\mathrm{m\,s}^{-1}$. The red shaded zones correspond to the times of the three transects. Bars at the top of each frame mark the calculated positions of the inner front.

Table 2
Characteristics of the inner front

Grid name/Date	Line ID	Middle shelf regime characteristics						Cold belt	Inner front dimensions		
		T (°C) upper 5 m	Sal (psu) upper 5 m	T (°C) lower 5 m	Sal (psu) lower 5 m	Thermocline depth (m)	Steepest dT/dz (°C/m)	T-surface min (°C)	Dist. coast: outer edge (km)	Dist. coast: inner edge (km)	Frontal width (km)
Nunivak I.											
17 June 1997	nie	4.55	30.8	0.33	30.9	×	×		183	56	127
17 June 1997	nic1	3.97	30.8	0.48	30.8	×	×		175	×	
18 June 1997	nib					20	−0.96		×	×	
18 June 1997	nia	5.17	30.8	0.33	30.9	20	−1.17		175	×	
19–20 June 1997	nic2	5.70	31.0	0.69	31.2	23	−1.72	3.72	184	63	121
28–29 Aug. 1997	nia1	10.80	31.1	1.88	31.4	27	−1.82		×	×	
29 Aug. 1997	nib	10.30	30.7	2.84	30.8	20	−2.26		143	×	
29 Aug. 1997	nic1	10.30	30.7	2.29	30.8	20	−2.74		145	×	
29 Aug. 1997	nid	10.10	30.7	3.54	30.9	20	−1.31		142	×	
30 Aug. 1997	nie	10.10	30.7	3.33	30.9	19	−1.49	7.93	153	105	48
2–3 Sept. 1997	nic2	8.50	30.8	1.96	31.0	25	−1.42	7.11	170	136	34
3–5 Sept. 1997	nia2	8.04	30.8	2.51	31.0	26	−2.04	7.39	165	135	30
14 June 1998	nic1	5.42	31.8	2.42	32.0	29	−0.75		200	162	38
16–17 June 1998	nic2	4.10	31.6	2.18	32.0	29	−0.75	2.67	176	146	30
25 Aug. 1998	nic1	6.39	31.9	3.4	31.9	32	−1.27	6.20	179	×	25
26–27 Aug. 1998	nia	6.12	31.9	3.35	31.9	33	−1.17	6.08	165	140	30
27 Aug. 1998	nie	6.99	32.0	3.38	32.0	34	−1.61	6.16	164	134	44
29–30 Aug. 1998	nic2	6.96	32.1	3.66	32.1	30	−2.10	6.19	169	125	
6–7 June 1999	nia	0.84	31.7	−0.36	31.7	28	−0.65	−0.07	180	165	15
5–6 June 1999	nic1	0.53	31.7	−0.77	31.7	33	−0.32	0.06	174	169	5
7 June 1999	nic2	3.09	31.9	0.55	32.3	24	−0.83		189	×	
6 June 1999	nie	1.02	31.7	−0.65	31.9	24	−0.40	0.07	173	158	15
11–12 Aug. 1999	nic1	7.51	31.8	2.90	32.4	24	−2.01	5.53	164	145	19
14 Aug. 1999	nic2	7.19	31.9	2.10	31.7	29	−2.15	6.09	162	140	22
14 Aug. 1999	nia	8.04	31.9	1.70	31.9	30	−2.22	6.03	164	×	
15 Aug. 1999	nie	7.88	32	1.88	32.0	24	−2.28	×	162	×	
15–16 Aug. 1999	nic3	8.01	31.9	1.96	32.0	21	−2.08	6.05	173	140	33
Cape Newenham											
12 June 1997	cne	7.06	31.2	1.64	31.2	12	−1.02	4.58	112	72	40
13–14 June 1997	cnc	6.80	31.2	1.26	31.3	9	−2.09		107	29	78
6 June 1998	cna	4.62	31.9	3.35	32.0	×	×		164	148	16
6 June 1998	cnc1	4.83	32.0	3.44	32.0	×	×	2.87	156	151	5
6–7 June 1998	cne	3.29	31.6	3.25	31.6	31	−0.41	3.09	163	154	9

Date	Station										
11 June 1998	cnc2	5.32	31.9	2.97	32.0	×	×		161	×	112
31 Aug.–1 Sept. 1998	cnc2	7.86	31.9	4.58	31.9	32	−2.02	7.54	161	49	33
1–2 June 1999	cne					×	×		×	156	25
6 Aug. 1999	cnc1	7.88	31.8	1.42	31.8	24	−2.96	6.03	145	112	
7–8 Aug. 1999	cnc2	8.10	31.8	1.35	31.8	24	−2.33	6.05	142	117	
Port Moller											
9 June 1997	pma	6.96	31.7	2.81	31.8	12	−1.28	5.39	35	×	
9–10 June 1997	pmc	7.63	31.8	2.61	31.8	11	−1.10	5.03	26	×	
10 June 1997	pme	7.95	31.8	2.66	31.8	10	−1.85		44	×	
26 May 1999	pme					×	×	−0.38	×	×	
2 Aug. 1999	pma	8.13	31.4	3.55	31.5	15	−0.9	7.86	25	×	
1 Aug. 1999	pmc	7.47	31.4	3.56	31.5	18	−0.98		20	×	
1 Aug. 1999	pme	7.55	31.4	3.16	31.5	18	−1.11		24	7	17
Slime Bank											
1–2 June 1997	sbc1	7.26	31.9	2.53	32.0	9	−0.52	5.20	13	6	7
2 June 1997	sbe	6.49	31.9	2.36	32.0	13	−0.45	5.27	30	5	24
2 June 1997	sbd	7.66	31.9	2.42	32.0	11	−0.62	5.43	18	16	2
3 June 1997	sbb	7.37	31.9	2.74	32.0	12	−0.58		29	×	
1											
3 June 1997	sba1	7.57	31.7	3.78	31.8	11	−0.85	×	6	×	
5 June 1997	sba2	7.52	31.9	2.78	32.0	11	−1.20	5.46	6	×	
10 Sept. 1997	sbc	10.00	31.8	5.88	32.7	×	×	9.83	33	8	25
9 Sept. 1997	sbe	10.40	31.8	6.57	32.6	×	×		35	10	25
27 May 1998	sbe					×	×	<0.5°	×	33	
27 May 1998	sbc1					×	×	<0.5°	×	20	
19 June 1998	sbc2	6.77	31.9	5.59	32.0	36	−1.03	<0.5°	32	11	22
20 Aug. 1998	sbc	10.6	32.3	5.28	32.3	×	×	8.95	32	11	22
20 Aug. 1998	sba	10.6	32.5	5.44	32.5	×	×	9.55	45	23	23
20 Aug. 1998	sbe	9.75	32.3	5.60	32.3	33	−0.21	9.05	30	6	24
14 June 1999	sbc2	5.08	31.9	3.46	32.2	18	−0.62	4.81	34	×	
27–28 July 1999	sbe1	9.14	32.0	5.11	32.7	33	−0.36	8.04	20	×	
28 July 1999	sbc	8.66	32.0	3.95	32.4	14	−0.49	7.99	25	×	
28 July 1999	sba	8.74	32.0	3.95	32.4	×	×				
30 July 1999	sbe2	8.81	32.0	4.54	32.5	×	×	8.01		25	×

(Fig. 3, lower right). In the coastal domain and in the surface waters of the middle shelf domain nutrients were nearly depleted, while the cold pool retained high concentrations. At the inner front, vertical, finger-like structures with elevated concentrations of nitrate coincided with the 5.5°C isotherm (Fig. 9, top panel). Other instances of similar patterns were observed at all the areas sampled in August 1998 and at Cape Newenham in June 1998 (Fig. 4). Transects at Slime Bank also exhibited enhanced nitrate at or near the surface associated with the inner front (in May 1997 and 1999, and August 1998 and 1999, Fig. 5).

The supply of nutrients and the resultant primary production on the southeastern Bering Sea shelf are highly sensitive to weather events, such as the timing of sea-ice cover and individual storm events that vertically mix the water column. Stabeno et al. (2001) observed a series of events in the spring of 1997 that depleted the main reservoir of nutrients over the shelf. An early spring ice-edge bloom that utilized nutrients in the upper water column was followed by an unusually large storm in mid-May that mixed waters to a depth of 50 m over the shelf. The unused nutrients from the lower layer were redistributed throughout the water column, which initiated a secondary bloom. Calm winds and strongly positive solar heating anomalies from late May to mid-July (Overland et al., 2001) led to a shallow mixed layer and sufficient light penetrating the thermocline to permit primary production and nutrient draw-down within the bottom waters. By June, the entire water column was essentially nutrient depleted across the middle shelf—a condition that persisted into early September.

Evidence for the importance of wind mixing to nutrient replenishment is provided in the transects from Nunivak Island in August 1998, and Cape Newenham in both 1998 and 1999. Immediately prior to the transects, storms caused nutrients from below the thermocline to be mixed into the surface layer, where they could support primary production. Measurements of higher levels of fluorescence coinciding with elevated nitrate concentrations both over the cool pool and near the inner front, imply that primary production was occurring there (Fig. 2).

5. Discussion

Based on observations collected during the IFP, our knowledge of the inner front has been significantly enhanced. Previous research (e.g., Muench, 1976; Schumacher et al., 1979; Coachman, 1986) gave only a basic description of the inner front. Our results provide a more thorough description and new understanding of the mechanisms that modify this feature, which is critical to the ecosystem of the southeastern Bering Sea shelf. In addition, an improved method for defining its location and lateral extent has been constructed. Marked spatial variability in frontal characteristics exists between the inner front along the Aleutian Peninsula and those on the broader shelf off Cape Newenham and Nunivak Island. This variability is caused by regional differences in forcing mechanisms.

On the broad shelf of the southeastern Bering Sea, wind and tidal mixing are the dominant processes defining the physical structure of the water column. In the coastal region, the water depth is sufficiently shallow (< 50 m) for the wind-mixed surface layer to overlap the bottom tidally mixed layer, resulting in a region with nearly uniform top-to-bottom water properties. During the summer, the middle shelf (50–100 m) is characterized by a warm surface mixed layer overlaying a colder, bottom tidally mixed layer. The warm surface layer becomes nutrient-depleted, while the bottom "cold pool," in most years, acts as a reservoir with higher nutrient concentrations. Separating the middle-shelf regime from the well-mixed coastal regime is the inner front, whose position varies depending on the strength of both the wind and tidal mixing and the depth of the water. Contrary to earlier hypothesis (Schumacher et al., 1979), the position of the inner front is not tied to the bottom slope. Within the inner front, a cold belt marks the location where potentially nutrient-rich waters from the cold pool mix with the waters of the surface layer. The occurrence of a cold belt, which is located just shoreward of the two-layer middle shelf regime, can be explained by a combination of spatially constant solar heating and wind mixing acting on waters of changing bottom depth. The lowered SST of the cold belt marks the region where

near-surface nutrient enrichment at the front was observed.

Along the Alaska Peninsula the structure of the inner front can be modified by proximity to both the coast and to Unimak Pass, a source of water with more oceanic characteristics (Stabeno et al., 2002). Relatively warm freshwater plumes can be advected over the position of the front, thereby inhibiting vertical mixing and shutting down its functioning as a nutrient pump. Alternatively, advection of oceanic water from Unimak Pass breaks down the two-layered mid-shelf structure and is a source of nutrients to Slime Bank. Occasional winds from the southeast provide the necessary conditions for upwelling.

The southeastern Bering Sea shelf is a region characterized by strong interannual variability (Stabeno et al., 2001; Schumacher et al., in press). Differences in initial (springtime) water properties and physical forcing mechanisms (ice advance/ retreat of sea ice and storm strength and timing) result in marked interannual variations in the biophysical features of the inner front. Each of the years of this study (1997–1999) presented a different combination of the timing of ice retreat, storm events, initial thermal conditions, and heat flux.

Interannual variability in wind and ice conditions created differences in the effectiveness of processes at the inner front that pump nutrients from the bottom layer toward the surface. In 1997 the nutrient supply in the cold pool was depleted by two factors: a May storm that mixed up nutrients from below the thermocline; and a photic depth deeper than the mixed-layer depth, which permitted primary production to take place in the bottom layer (Rho, 2000; Stockwell et al., 2001). Unusually weak winds moved the front shoreward. By late August when storm winds did break down the stratification and set up the inner front farther seaward, no nutrients were available to mix upward. As a result of these factors, prolonged primary production did not occur at the inner front, which may have exacerbated the conditions that led to a die-off of short-tailed shearwaters (*Puffinus tenuirostris*) in August 1997 (Baduini et al., 2001; Napp and Hunt, 2001; Hunt et al., 2001). In 1998, ice was present only briefly during February, a time of weak wind mixing. The water

column did not cool to the bottom (Stabeno et al., 2001), which led to the formation of a cool pool (2.5–4°C) over the middle shelf, rather than a cold pool (<2°C). Frequent strong winds throughout the spring and summer sustained a mixed layer near 30 m deep and delayed the onset of the spring bloom. As a result of these factors, the highest levels of nutrients we observed occurred in June 1998. In 1999, ice did not melt at the Nunivak Island grid until June, which delayed warming of the upper mixed layer.

Individual weather events were observed to have dramatic impacts on the hydrographic structure within just a few days. One storm event in 1997 cooled the surface layer by 2°C within 3 days and deepened the mixed layer by 7–10 m. Calm weather for a week after a storm in 1999 caused a warming of water temperatures above the cold pool and in the coastal domain, as well as a widening of the inner front from 19 to 31 km within 4 days. A storm at the beginning of August 1999 deepened the wind-mixed upper layer, and slightly increased nitrate concentrations over the cold pool on the Cape Newenham transect. Within a few days, vertical filaments or finger structures developed in the inner front off Nunivak Island. These had colder temperatures and higher nutrient concentrations than the surrounding waters. These transects best illustrate the conditions whereby processes at the inner front supply nutrients to the upper layer, thus prolonging production.

Our set of observations demonstrate that it is impossible to characterize a summer season in this area with a single set of transects, or even transects at multiple locations, since weather events significantly impact the distribution of physical and chemical properties within short periods of time. While CTD/nutrient transects are necessary to resolve spatial patterns (i.e. location and width of the front, mixed layer depth, extent of the cold (cool) pool), they must be used in conjunction with bio-physical moorings that provide temporal data to measure this environment with sufficient accuracy to characterize changes that may be taking place and to provide information needed for fisheries management.

Observations confirm the hypothesis that pumping of nutrients into the euphotic zone does occur

and can prolong primary production at the inner front of the eastern Bering Sea shelf. The effectiveness of this process depends on two factors: the existence of a reservoir of nutrients in the lower layer of the middle shelf; and the occurrence of sufficient wind mixing to break down surface layer stratification. The frontal area with its weaker stratification than that over the cold pool is more susceptible to wind mixing. Intensification of either wind or tidal mixing (through its fortnightly cycle) moves the inner front seaward, where a reservoir of nutrients usually is located in the cold/cool pool. When this occurs, nutrients mix upward, where they can be utilized by the phytoplankton. While our observations have significantly improved knowledge of the inner front, they do not include two mechanisms that are integral to inner front biophysical dynamics (Coachman, 1986). How important are internal tides that perturb the pycnocline, creating waves that make nutrients more available to the euphotic zone via weak mixing events, and what are the processes that transport nutrients onto the middle shelf? The answers to these questions would make it possible to understand the biophysical sequence of events that regulates bottom-up control of overall production on this shelf.

Acknowledgements

References

Baduini, C.L., Hyrenbach, K.D., Coyle, K.O., Pinchuk, A., Mendenhall, V., Hunt Jr., G.L., 2001. Mass mortality of short-tailed shearwaters in the eastern Bering Sea during summer 1997. Fisheries-Oceanography 10 (1), 117–130.
Chen, C., Beardsley, R.C., 1998. Tidal mixing and cross-frontal particle exchange over a finite amplitude asymmetric band: a model study with application to George Bank. Journal of Marine Research 56, 1163–1201.
Coachman, L.K., 1986. Circulation, water masses, and fluxes on the southeastern Bering Sea shelf. Continental Shelf Research 5, 23–108.
Decker, M.B., Hunt Jr., G.L., 1996. Foraging by murres (Uria spp.) at tidal fronts surrounding the Pribilof Islands, Alaska, USA. Marine Ecology Progress Series 139, 1–10.
Fearnhead, P.G., 1975. On the formation of fronts by tidal mixing around the British Isles. Deep-Sea Research 22 (11), 311–321.
Franks, P.J.S., Chen, C., 1996. Plankton production in tidal fronts: a model of Georges banks in the summer. Journal of Marine Research 54, 631–651.
Gaard, E., Hansen, B., Heinesen, S.P., 1998. Phytoplankton variability on the Faroe Shelf. ICES Journal of Marine Sciences 55, 688–696.
Geyer, W.R., 1995. Tide-induced mixing in the Amazon frontal zone. Journal of Geophysical Research 100 (2), 2341–2353.
Hattori, A., Goering, J.J., 1981. Nutrient distributions and dynamics in the eastern Bering Sea. In: Hood, D.W., Calder, J.A. (Eds.), The eastern Bering Sea Shelf: oceanography and resources, Vol. 2. NOAA/OMPA. Distributed by University of Washington, Seattle, WA, pp. 975–992.
Haung, D.J., Su, J.L., Backhaus, J.O., 1999. Modeling the seasonal thermal stratification and baroclinic circulation in the Bohai Sea. Continental Shelf Research 19 (11), 1485–1505.
Hunt Jr., G.L., Colye, K.O., Hoffman, S., Decker, M.B., Flint, E.N., 1996. Foraging ecology of short-tailed shearwaters near the Pribilof Islands, Bering Sea. Marine Ecology Progress Series 141, 1–11.
Hunt Jr., G.L., Baduini, C.L., Coyle, K., Pinchuk, A., 2001. Changes in diet and body condition of shearwaters in response to changing euphausiid populations in the Southeastern Bering Sea. Deep-Sea Research II: Topical Studies in Oceanography, this issue.

Kasai, A., Rippeth, T.P., Simpson, J.H., 1999. Density and flow structure in the Clyde Sea front. Continental Shelf Research 19 (14), 1833–1848.

Kinder, T.H., Schumacher, J.D., 1981. Hydrographic structure over the continental shelf of the southeastern Bering Sea. In: Hood, D.W., Calder, J.A. (Eds.), The Eastern Bering Sea Shelf: Oceanography and Resources. University of Washington Press, Seattle, pp. 31–52.

Kinder, T., Hunt Jr., G.L., Schneider, D., Schumacher, J.D., 1983. Oceanic fronts around the Pribilof Islands, Alaska: correlations with seabirds. Estuarine, Coastal and Shelf Science 16, 309–319.

Lie, H.J., 1988. Tidal fronts in the southeastern Hwanghae (Yelloe Sea). Continental Shelf Research 9 (6), 527–546.

Loder, J.W., Brickman, D., Horne, E.P.W., 1992. Detailed structure of currents and hydrography on the northern side of Georges Bank. Journal of Geophysical Research 97 (9), 14,331–14,551.

Muench, R.D., 1976. A note on eastern Bering Sea shelf hydrographic structure: August 1974. Deep-Sea Research 23, 245–247.

Napp, J.M., Hunt Jr., G.L., 2001. Anomalous conditions in the Southeastern Bering Sea, 1997: linkage among climate, weather, ocean and biology. Fisheries-Oceanography 10 (1), 61–69.

Overland, J.E., Salo, S.A., Kantha, L.H., Clayson, C.A., 1999. Thermal stratification and mixing on the Bering Sea shelf. In: Loughlin, T.R., Ohtani, K. (Eds.), Dynamics of the Bering Sea: A Summary of Physical, Chemical, and Biological Characteristics, and a Synopsis of Research on the Bering Sea. Alaska Sea Grant College Program, Fairbanks, AK, pp. 129–146.

Overland, J.E., Bond, N.A., Miletta, J., 2001. North Pacific atmospheric and SST anomalies in 1997: Links to ENSO? Fisheries-Oceanography 10 (1), 69–80.

Pingree, R.D., Griffiths, D.K., 1978. Tidal fronts on the shelf seas around the British Isles. Journal of Geophysical Research 83 (9), 4615–4622.

Reed, R.K., Stabeno, P.J., 2003. Surface heat fluxes and subsurface heat content at a site over the southeastern Bering Sea shelf, May–July 1996. Deep-Sea Research II, this issue (PII: S0967-0645(02)00325-9).

Rho, T.K., 2000. Carbon and nitrogen uptake dynamics during 1997 and 1998 anomalous conditions in the Bering Sea. M.S. Thesis, School of Fisheries and Ocean Sciences, University of Alaska Fairbanks, Fairbanks, 95pp.

Sambroto, R.N., Niebauer, H.J., Goering, J.J., Iverson, R.L., 1986. Relationships among vertical mixing, nitrate uptake and phytoplankton growth during the spring bloom in the southeast Bering Sea middle shelf. Continental Shelf Research 5, 161–198.

Schumacher, J.D., Kinder, T.H., 1983. Low-frequency current regimes over the Bering Sea shelf. Journal of Physical Oceanography 13, 607–623.

Schumacher, J.D., Stabeno, P.J., 1998. Continental shelf of the Bering Sea. In: The Sea: Vol. 11, The Global Coastal Ocean: Regional Studies and Synthesis. Wiley, New York, NY, pp. 789–822.

Schumacher, J.D., Kinder, T.H., Pashinski, D.J., Charnell, R.L., 1979. A structural front over the continental shelf of the eastern Bering Sea. Journal of Physical Oceanography 9, 79–87.

Schumacher, J.D., Pearson, C.A., Overland, J.E., 1982. On exchange of water between the Gulf of Alaska and the Bering Sea through Unimak Pass. Journal of Geophysical Research 87, 5785–5795.

Schumacher, J.D., Bond, N.A., Brodeur, R.D., Livingston, P.A., Napp, J.M., Stabeno, P.J., 2002. Climate change in the Southeastern Bering Sea and some consequences for biota. In: Hempel, Sherman (Eds.), Large Marine Ecosystems of the World: Trends in Exploitation, Protection and Research, in press.

Semenov, C.V., Luneva, M.V., 1999. Combined effect of tide, stratification, and vertical turbulent mixing on the formation of hydrophysical fields in the White Sea. Izvestiya Akademii Nauk Fizika Atmosfery I Okeana 35 (5), 660–678.

Simpson, J.H., Hunter, J.R., 1974. Fronts in the Irish Sea. Nature 250, 404–406.

Stabeno, P.J., Bond, N.A., Kachel, N.B., Salo, S.A., Schumacher, J.D., 2001. Temporal variability in the physical environment over the southeastern Bering Sea. Fisheries-Oceanography 10 (1), 81–98.

Stabeno, P.J., Reed, R., Napp, J.M., 2002. Transport through Unimak Pass, Alaska. Deep-Sea Research II, this issue (PII: S0967-0645(02)00326-0).

Stockwell, D.A., Whitledge, T.E., Zeeman, S.I., Coyle, K.O., Knapp, J.M., Brodeur, R.D., Pinchuk, A.I., Hunt Jr., G.L., 2001. Anomalous conditions in the south-eastern Bering Sea, 1997: nutrients, phytoplankton and zooplankton. Fisheries-Oceanography 10, 99–116.

Takemouti, A.V., Ohtani, K., 1974. Currents and water masses in the Bering Sea: A review of Japanese work. In: Hood, D.W., Kelley, E.J. (Eds.), Oceanography of the Bering Sea. Occasional Publ. No. 2, Institute of Marine Science. University of Alaska, Fairbanks, Fairbanks, AK, pp. 39–57.

Whitledge, T.E., Luchin, V.A., 1999. Summary of chemical distributions and dynamics in the Bering Sea. In: Loughlin, T.R., Ohtani, K. (Eds.), Dynamics of the Bering Sea: A summary of Physical, Chemical, and Biological Characteristics, and a Synopsis of Research on the Bering Sea. University of Alaska Sea Grant, Fairbanks, AK, pp. 217–250.

Whitledge, T.E., Walsh, J.J., 1986. Biological processes associated with the thermocline and surface fronts in the Southeastern Bering Sea. In: Nihoul, J.C. (Ed.), Marine Interfaces Ecohydrodynamics. Proceedings of the 17th International Liege Colloquium on Ocean Hydrodynamics. Elsevier, Amsterdam, pp. 665–670.

Whitledge, T.E., Malloy, S.C., Patton, C.J., Wirich, C.D., 1981. A manual for nutrient analyses in seawater. Formal Report No. BNL 51398, Brookhaven National Laboratory, Upton, NY, 216pp.

Whitledge, T.E., Reeburgh, W.S., Walsh, J.J., 1986. Seasonal inorganic nitrogen distributions and dynamics in the southeastern Bering Sea. Continental Shelf Research 5, 109–132.